GBT MEMO 115

National Radio Astronomy Observatory
Charlottesville, Virginia 22903

GAIN REDUCTION DUE TO GRAVITY-INDUCED DEFLECTIONS OF THE GBT TIPPING STRUCTURE (Model 95, Version B) AND ITS COMPENSATION

S. Srikanth
September 9, 1994

Loss of gain as a result of gravity-induced deflections of the preliminary design of the tipping structure of the GBT was analyzed and presented in GBT Memo No. 78. The design of the tipping structure was finalized by Loral in December 1993. This design (Model 95, version B) meets both pointing and surface rms specifications at all elevation angles and weighs 9.39 million pounds. The rigging angle for this model is 43.8° elevation, where the main reflector is a paraboloid of focal length 60 meters. A finite element analysis of the tipping structure carried out using NASTRAN gives deflections of the main reflector surface, subreflector and feed attachment points for the antenna pointing at zenith and horizon. After fitting a parabola (different focal length) to the deflected main reflector surface, the surface rms, deflection of its vertex and rotation of the best-fit paraboloid with respect to the design paraboloid are computed. The deflections of the feed mounting point and subreflector vertex with respect to the best-fit paraboloid are also computed. These are given in Table 1. Figure 1 shows the coordinate systems used for the deflections presented in Table 1.

This memo presents calculation of gain loss and its compensation carried out for the Gregorian geometry. At prime focus, gain loss is marginal and its compensation by feed translation is straightforward. Computed far-field patterns of the telescope, using a diffraction program, at 43.8° elevation at four frequencies are shown in Figure 2. These patterns are in the symmetric plane of the antenna. Aperture efficiencies are tabulated in Table 2. Theoretical feed patterns have been used in these calculations. At any other elevation, there is deformation of the telescope. Deformation of the subreflector surface due to gravity is negligible and it is assumed that the subreflector is undeformed in all computations in this memo. In addition, rotations of the feed and subreflector are small and, hence, ignored. For the best-fit paraboloid, given the deflected positions of the subreflector and the feed, aperture efficiencies are calculated at horizon and zenith and presented in Table 3. Far-field patterns at horizon are shown in Figure 3 at 1.42 GHz and 20 GHz. Figure 4 shows the patterns at zenith. The telescope does not have a main beam at 20 GHz. As seen from Table 3, loss in aperture efficiency increases with increase in frequency. The loss is due to increased spillover and phase distortions in the aperture introduced by incorrect positions of the feed and the subreflector with respect to the best-fit paraboloid.

In order to separate the effects of spillover and phase distortions, a ray tracing program was used to analyze the deformed geometry. For the

geometry at horizon, out of a total of 1,117 rays, 19 missed the two reflectors, giving an efficiency loss of 0.06%. The distribution of path length variation, when tracing rays from the feed phase center to an aperture perpendicular to the telescope axis, is shown in Figure 5a. Path length errors through horizontal and vertical planes of the distribution are shown in Figures 5b and 5c. After fitting a plane to the distribution, the residual path length error is 4.46 mm. This indeed accounts for the large efficiency loss. There is no provision to translate the feed on the turret mount. Hence, any correction that needs to be applied is through translation and/or rotation of the subreflector. Given the best-fit paraboloid and the undeformed subreflector, the secondary focus position (S in Figure 6) for this combination is located. In Figure 6, S′ is the actual position of the focus of the subreflector, and F is the feed phase center location. In order to correct for the gain loss, the subreflector is first translated so that S′ coincides with the secondary focus S, identified above. The other focus of the subreflector does not coincide with the focus of the best-fit paraboloid because of the rotation of the best-fit surface indicated in Table 1. In addition, the feed is not at the secondary focus as shown in Figure 6. Columns 5 and 6 in Table 4 are the efficiency values for the cases of subreflector translations to the secondary focus positions at horizon and zenith, respectively. The loss in efficiency at horizon as compared to that at 43.8° elevation is 15.2% at 20 GHz. Ray tracing for this geometry gives spillover loss of 0.05%. Plots through horizontal and vertical planes of the path length distribution are shown in Figure 7. The residual path length error after fitting a plane is 0.49 mm, giving a phase efficiency of 84.54% at 20 GHz. This is consistent with the calculation done with the diffraction program.

By systematically translating the subreflector, the path length error is reduced to zero for the horizon case and to a very small value at zenith. The aperture efficiencies after correction are shown in Columns 7 and 8 of Table 4. The maximum leftover loss is 0.79% at 50 GHz. Figures 8 and 9 show the computed patterns after correction at horizon and zenith, respectively. The patterns at all frequencies have recovered very well and resemble those in Figure 2. At horizon the pointing error after correcting for gravity deformation is 1.6 arcminutes and at zenith 4.2 arcminutes. The subreflector translations, in the Y′ and Z′ directions (BFP coordinates), required for gain loss compensation are given in Table 6. Deflections of the elements of the telescope are linear functions of elevation and, hence, the geometry at any elevation can be obtained by interpolation of the values at the extremities.

TABLE 6. SUBREFLECTOR TRANSLATIONS

	Y′ (ins)	Z′ (ins)
Horizon	-4.056	-3.013
Zenith	6.374	-0.096

In conclusion, the gain loss of the GBT due to gravity deformations is almost entirely due to phase distortions in the aperture and correction can be applied by translation alone of the subreflector in most cases. The effort in this study is towards maximizing the gain of the telescope. The Mizugutch condition [1] is violated here due to the rotation of the best-fit surface. A future study will attempt to minimize cross-polarization by subreflector rotation in order to satisfy the Mizugutch condition. Deflections of the structure were provided by Lee King and the ray tracing program used in the analysis was developed by Roger Norrod.

[1] Y. Mizugutch, M. Akagawa and H. Yokoi, "Offset Dual Reflector Antenna," *1976 Int. IEEE/AP-S Symp. Digest*, pp. 2-4.

TABLE 1. GRAVITY-INDUCED DEFORMATIONS

	HORIZON			ZENITH		
BFP Parameters						
rms	0.040401			0.040428		
focal length	2362.38208 (60.0045 m)			2362.63428 (60.0109 m)		
wrt design paraboloid	X	Y	Z	X	Y	Z
BFP vertex deflection	0.0000	5.9102	1.2127	0.0000	0.4473	-1.0871
rotation (degrees)	0.045951			0.036383		
wrt to BFP axes	X′	Y′	Z′	X′	Y′	Z′
feed	0.0000	2.1602	3.0676	0.0000	-4.7007	1.0098
subreflector vertex	0.0000	3.9788	3.5757	0.0000	-6.4666	0.7246

TABLE 2. APERTURE EFFICIENCY (%) AT RIGGING ANGLE OF 43.8° ELEVATION

Freq. (GHz)	$\eta_{spo} * \eta_{ill}$	η_{rms}	η_a
1.42	71.7198	99.4479	71.3238
8.00	73.4662	83.8835	61.6260
20.00	76.0175	87.2793	66.3475
50.00	76.4016	83.9071	64.1064
Feed Taper ≤ 8.2 GHz - -15 dB; > 8.2 GHz - -13 dB.			
Surface rms ≤ 15 GHz - 0.049"; 15 to 43 Ghz - 0.017"; > 43 GHz - 0.0087".			

TABLE 3. APERTURE EFFICIENCY (%)

Freq. (GHz)	F = 60 m 44° Elev.	F = 60.0045 m At Horizon	F = 60.0109 m At Zenith
1.42	71.3238	70.4733	68.0635
8.00	61.6260	40.4142	14.5779
20.00	66.3475	0.4893	0.5604
50.00	64.1064	0.1988	0.3902

TABLE 4. APERTURE EFFICIENCY (%)

Freq. (GHz)	44° Elev.	Before Correction		Subrefl. at Optimum Position of Deformed Paraboloid		Subrefl. Translated for Minimum Phase Error	
		Horizon	Zenith	Horizon	Zenith	Horizon	Zenith
1.42	71.3238	70.4733	68.0635	71.2664 (0.1)	71.2352 (0.1)	71.3238	71.3238
8.00	61.6260	40.4142	14.5779	60.2885 (2.2)	60.9711 (1.1)	61.6260	61.6260
20.00	66.3475	0.4893	0.5604	56.2904 (15.2)	60.4080 (8.9)	66.3475	65.8500 (0.75)
50.00	64.1064	0.1988	0.3902	20.6934 (67.7)	36.1836 (43.6)	64.1064	63.6000 (0.79)

Numbers in parentheses are losses in efficiency as a percentage of column 2.

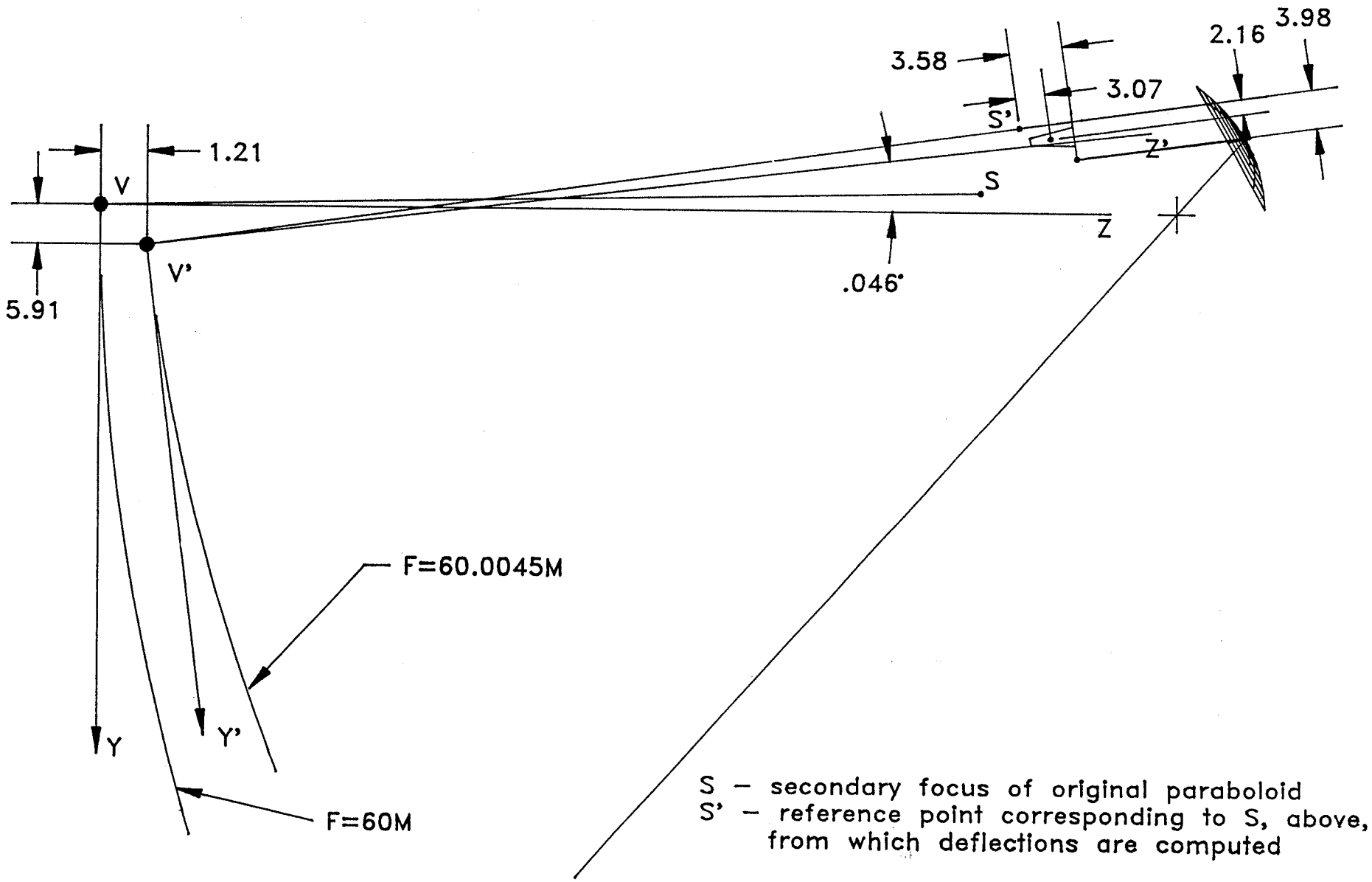

Fig. 1. Gravity–induced deflections at horizon.

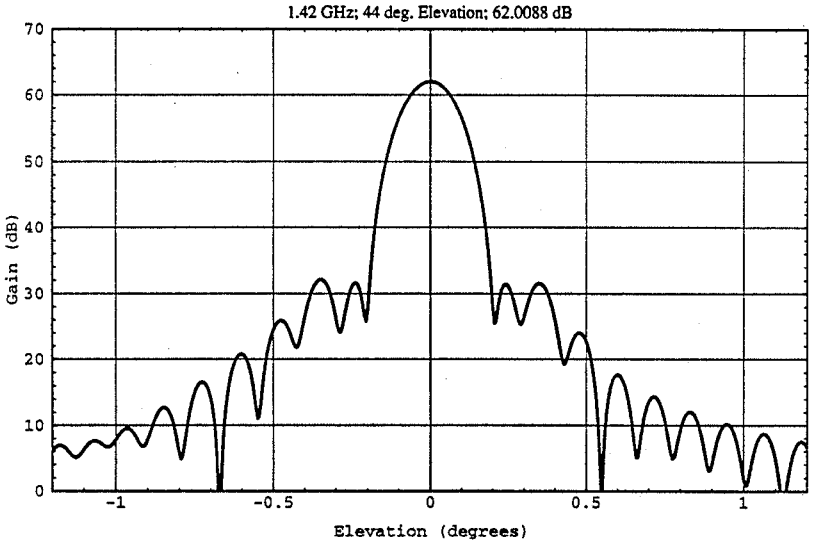

(a) 1.42 GHz

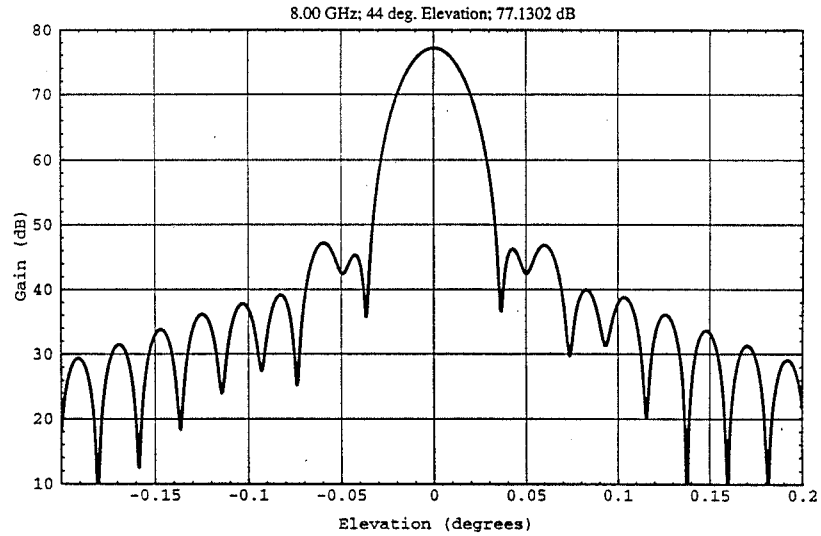

(b) 8.00 GHz

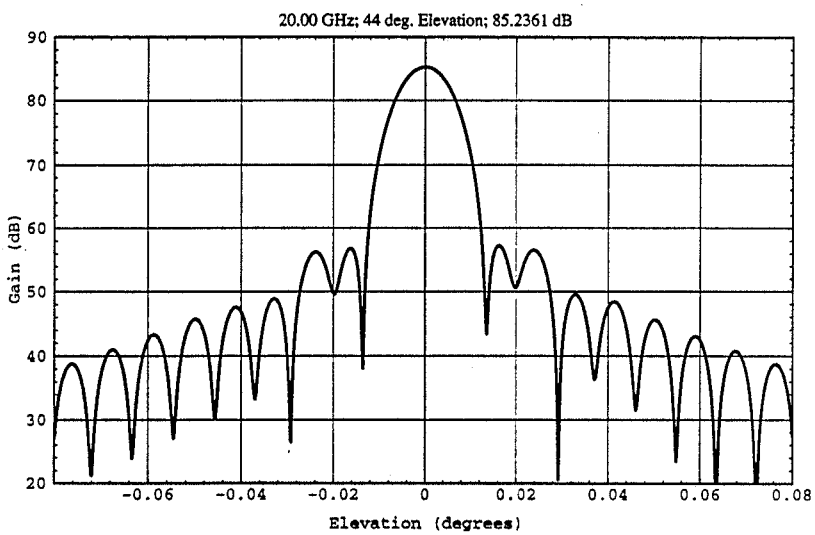

(c) 20.00 GHz

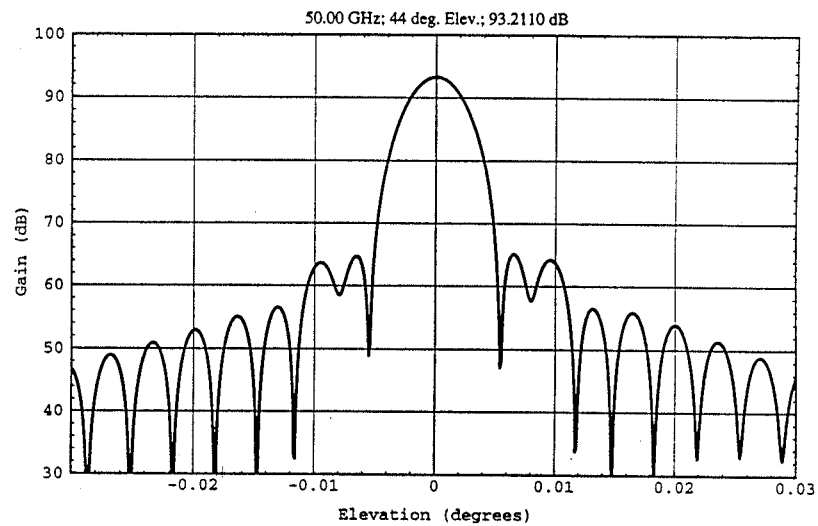

(d) 50.00 GHz

Fig. 2. Far-field patterns at 43.8° elevation (symmetric plane).

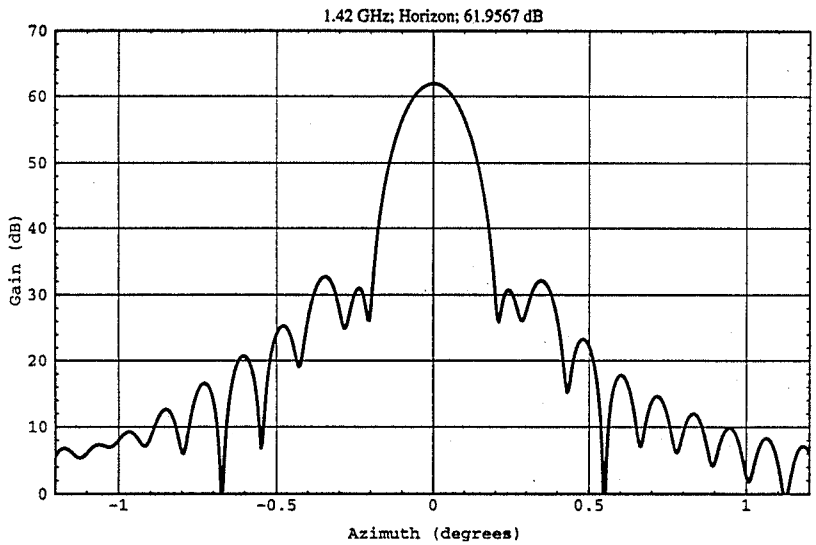

(a) 1.42 GHz
(Asymmetric plane)

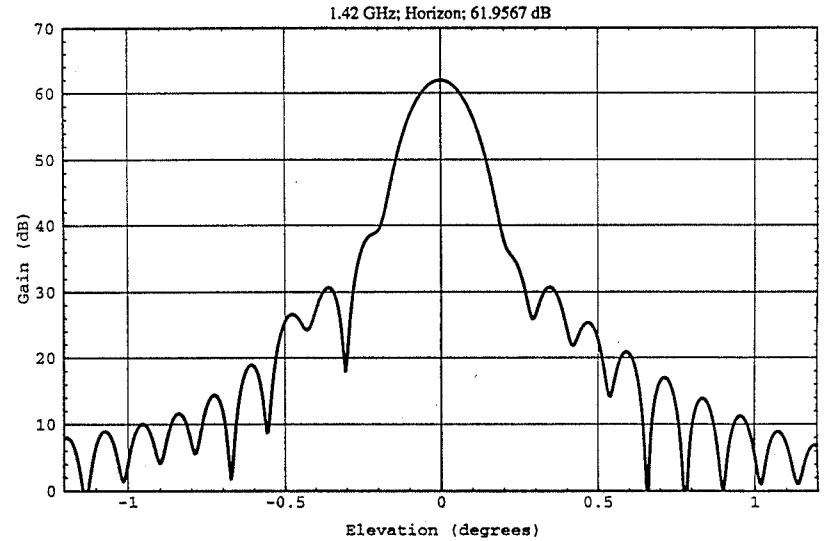

(b) 1.42 GHz
(Symmetric plane)

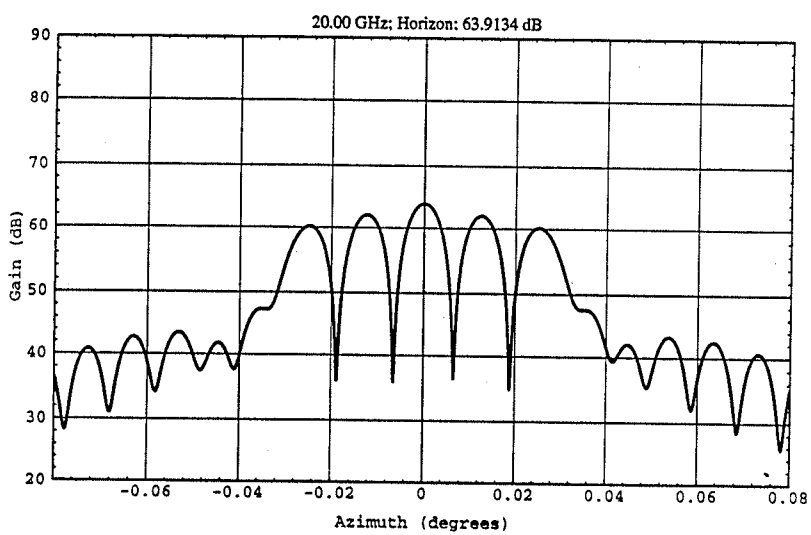

(c) 20.00 GHz
(Asymmetric plane)

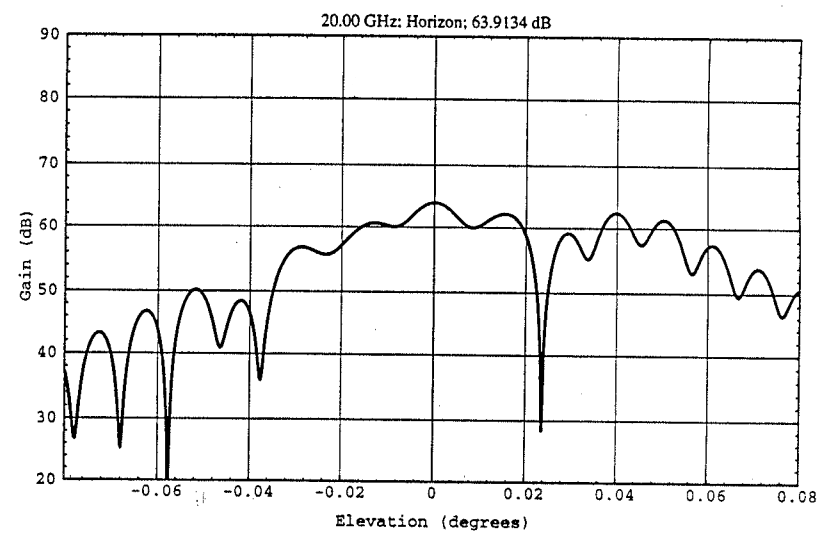

(d) 20.00 GHz
(Symmetric plane)

Fig. 3. Far-field patterns at horizon.

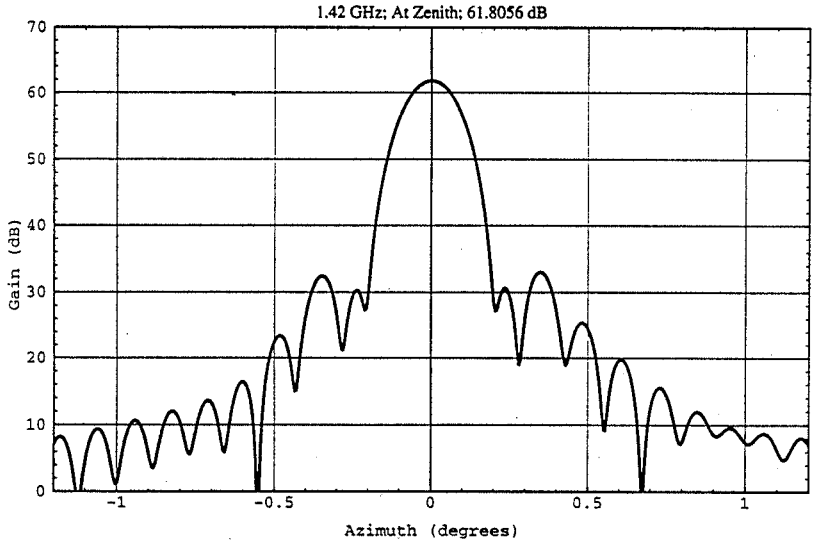

(a) 1.42 GHz
(Asymmetric plane)

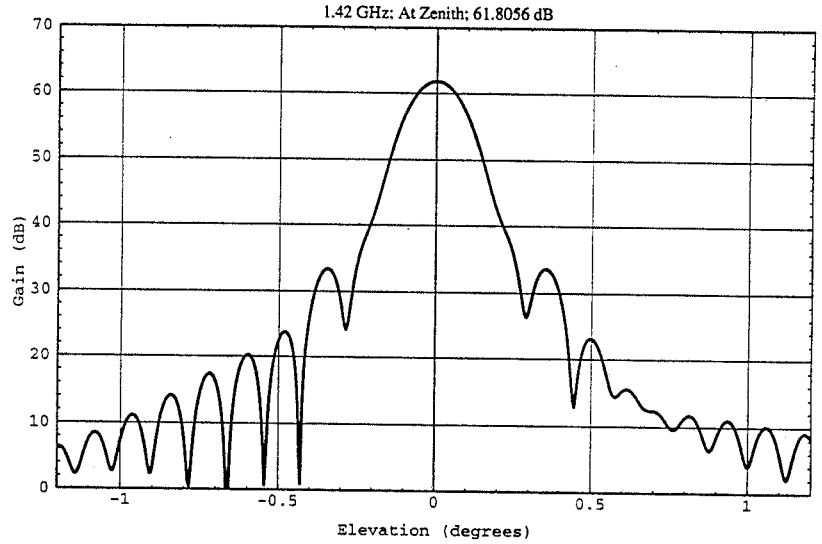

(b) 1.42 GHz
(Symmetric plane)

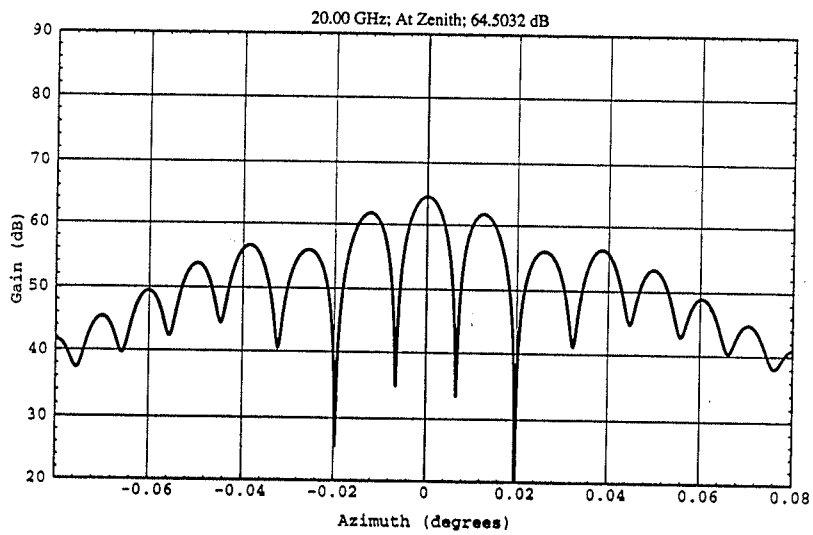

(c) 20.00 GHz
(Asymmetric plane)

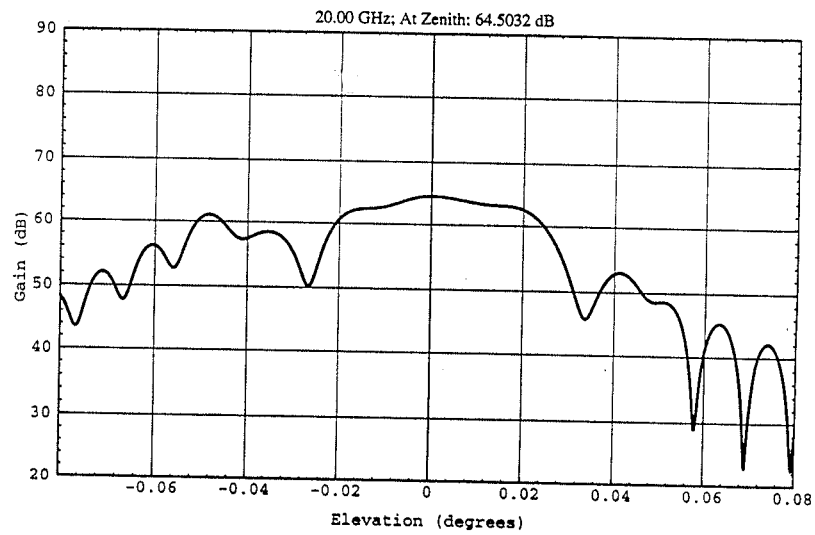

(d) 20.00 GHz
(Symmetric plane)

Fig. 4. Far-field patterns at zenith.

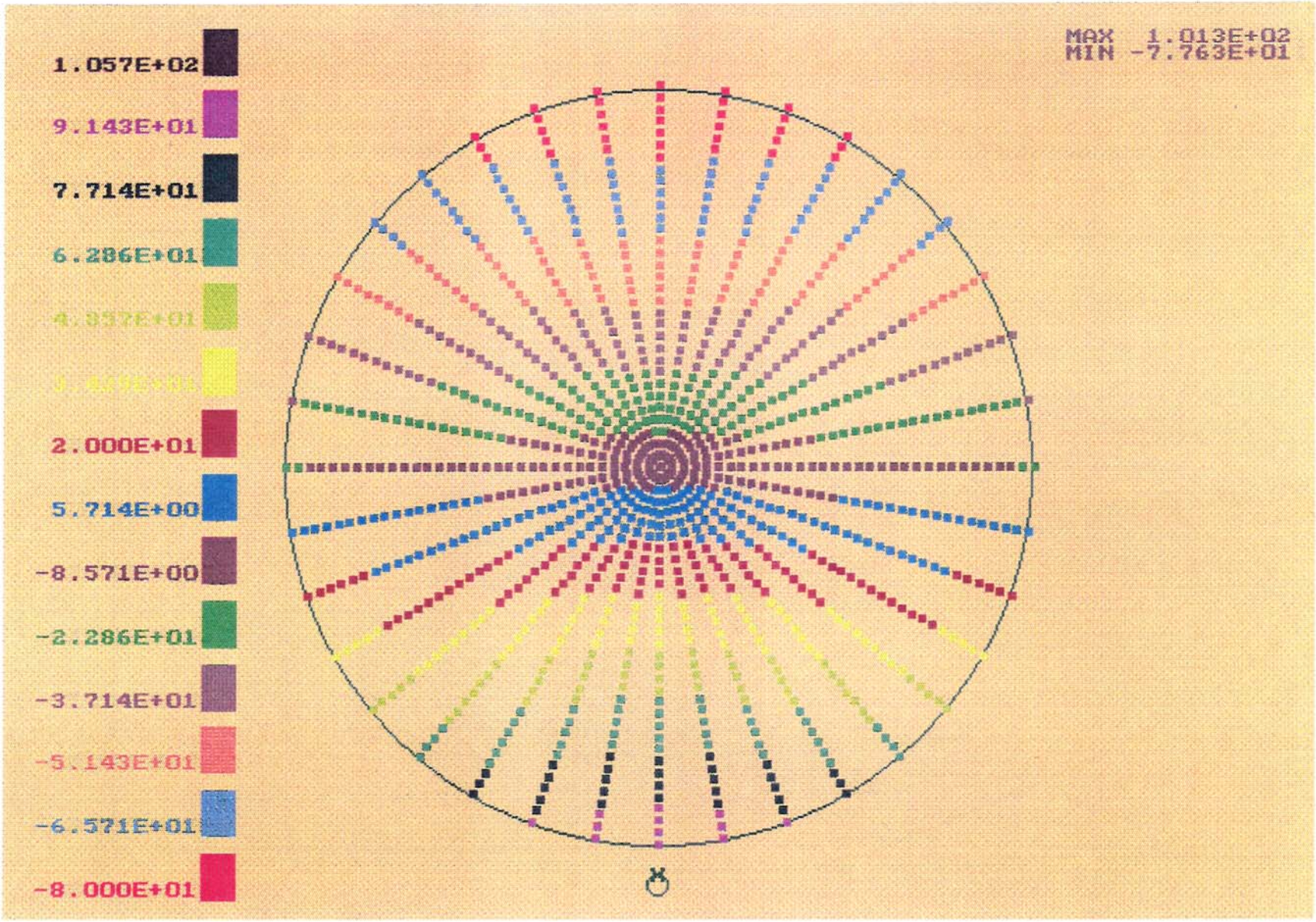

Fig. 5a. Aperture path length distribution (horizon, before correction).

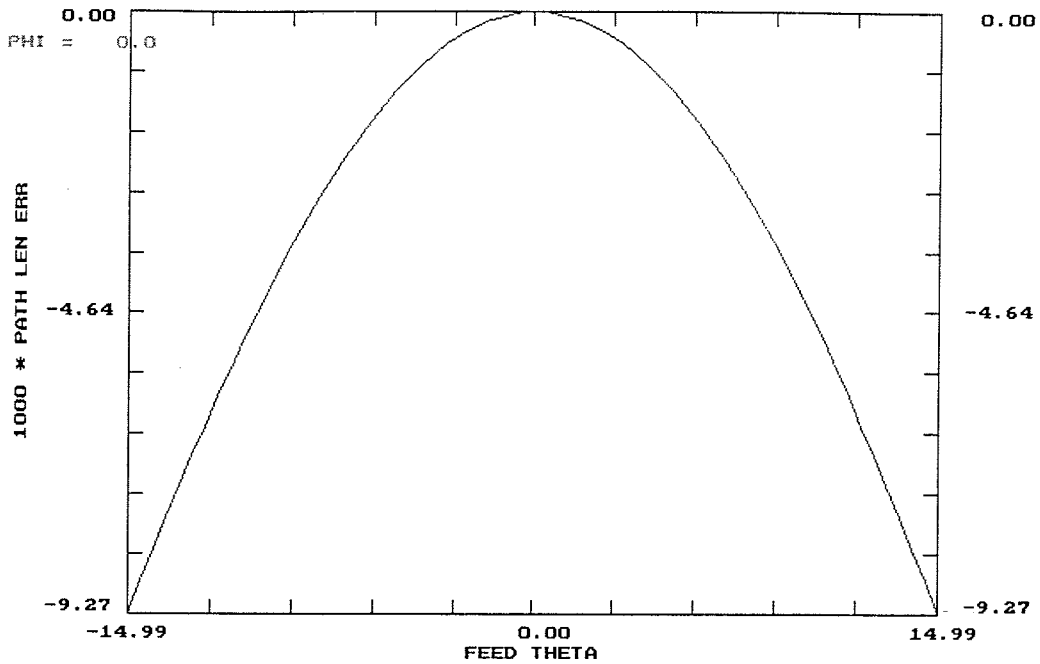

Fig. 5b. Aperture path length error in mm through horizontal plane (horizon, before correction).

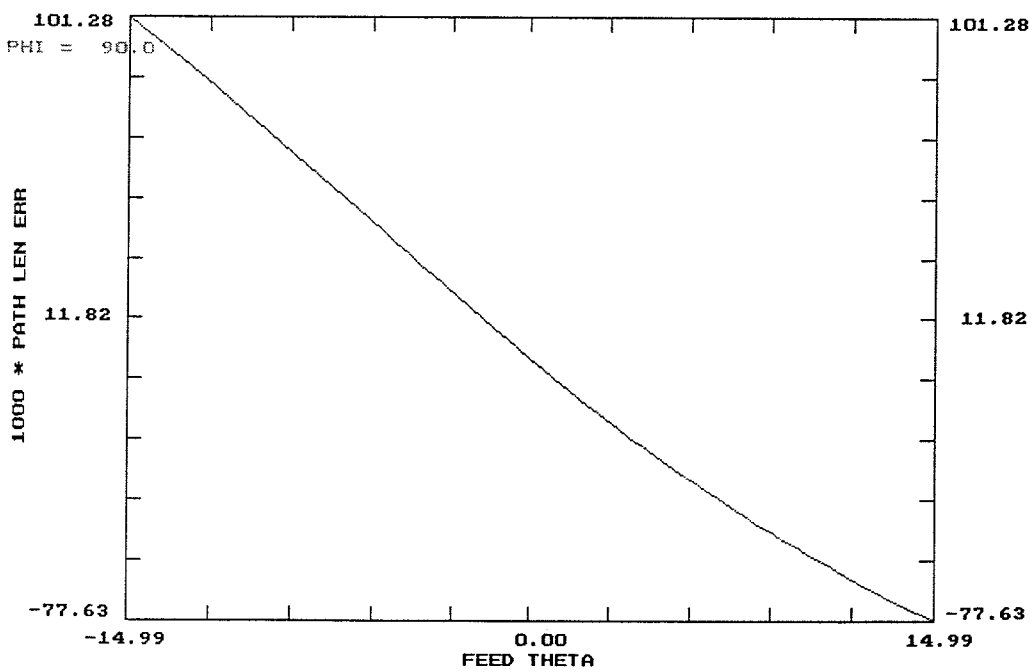

Fig. 5c. Aperture path length error in mm through vertical plane (horizon, before correction).

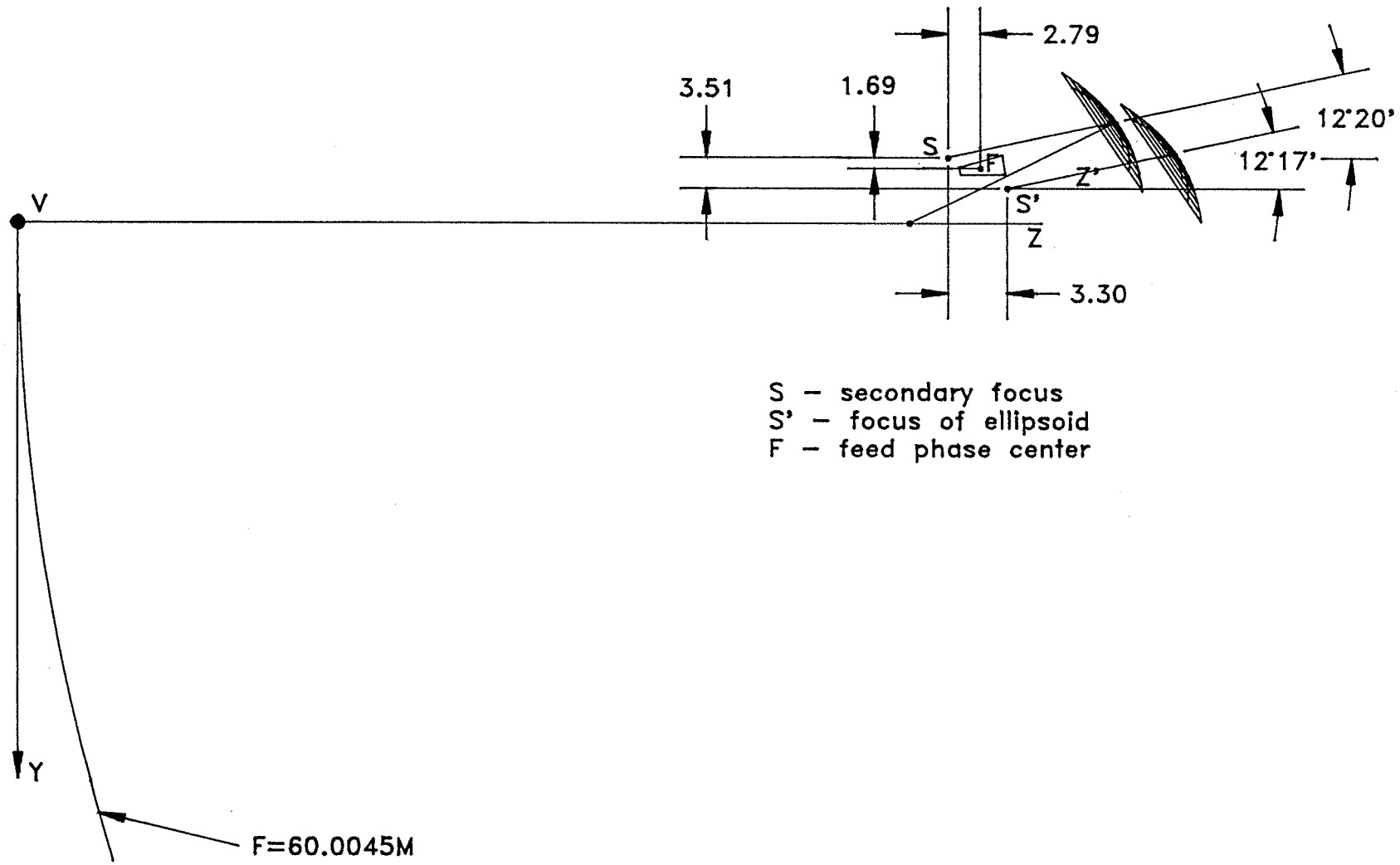

Fig. 6. Best–fit paraboloid at horizon.

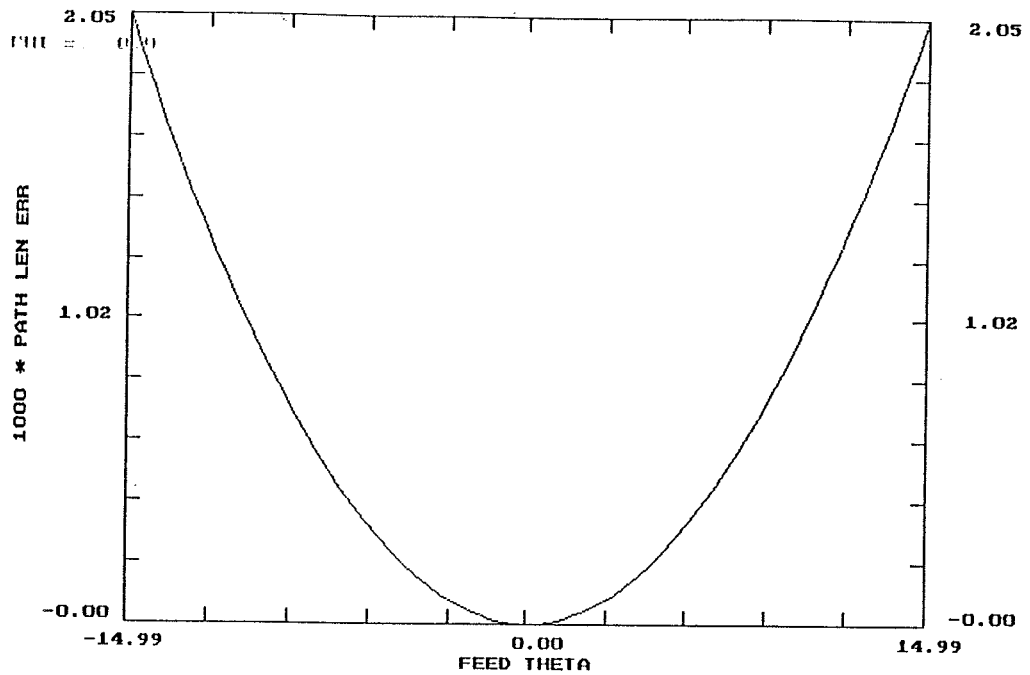

Fig. 7a. Aperture path length error in mm through horizontal plane (horizon, subreflector at secondary focus).

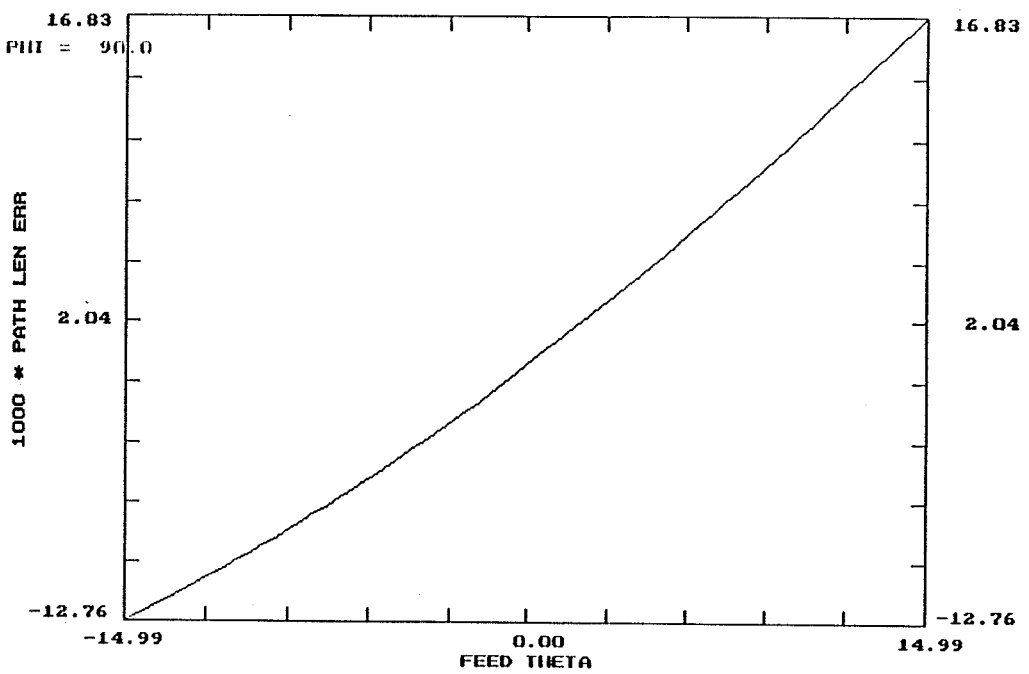

Fig. 7b. Aperture path length error in mm through vertical plane (horizon, subreflector at secondary focus).

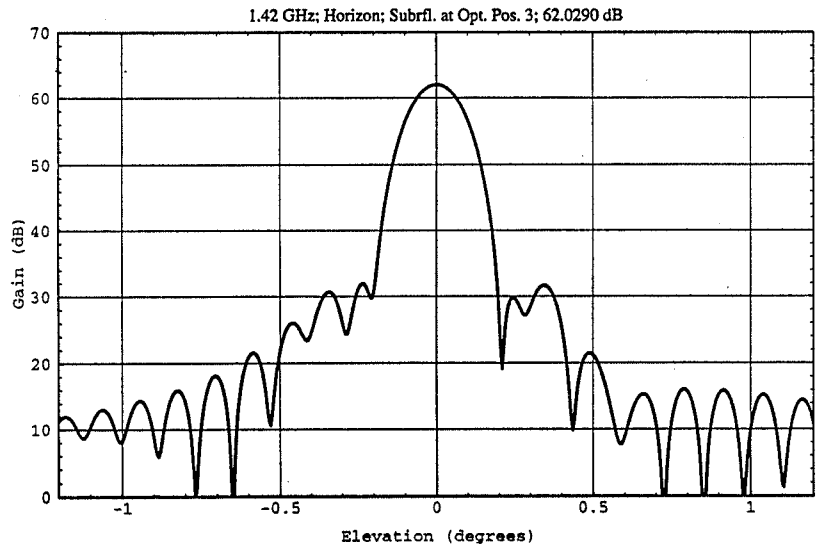

(a) 1.42 GHz

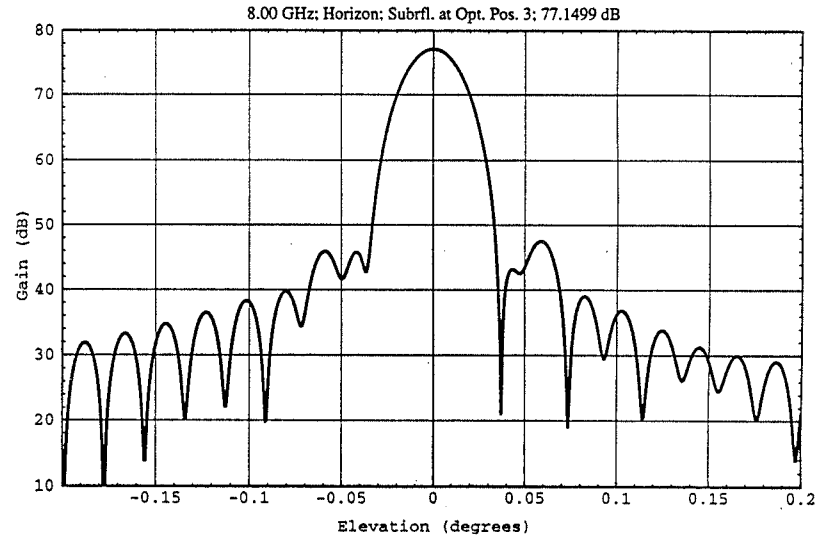

(b) 8.00 GHz

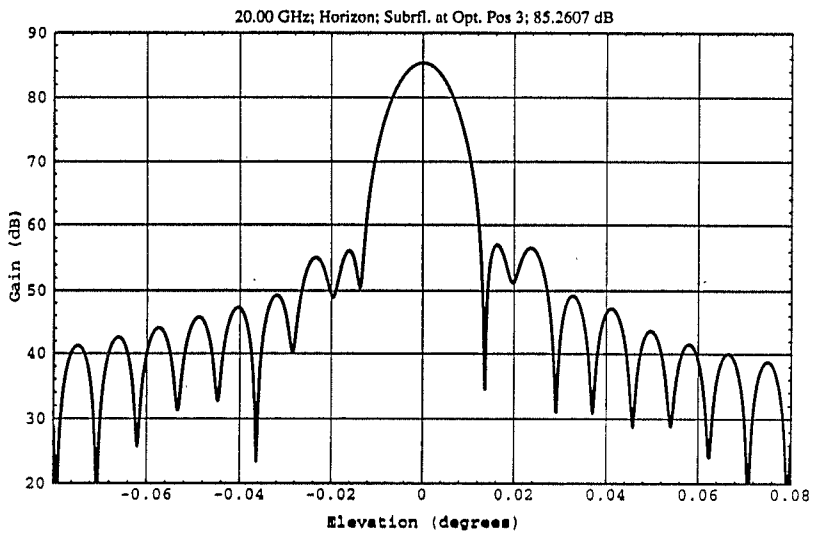

(c) 20.00 GHz

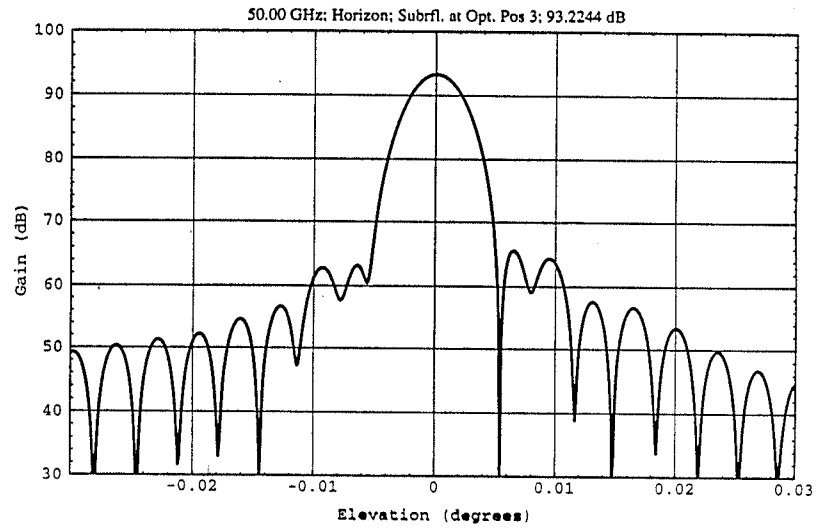

(d) 50.00 GHz

Fig. 8. Far-field patterns in the symmetric plane at horizon after correction.

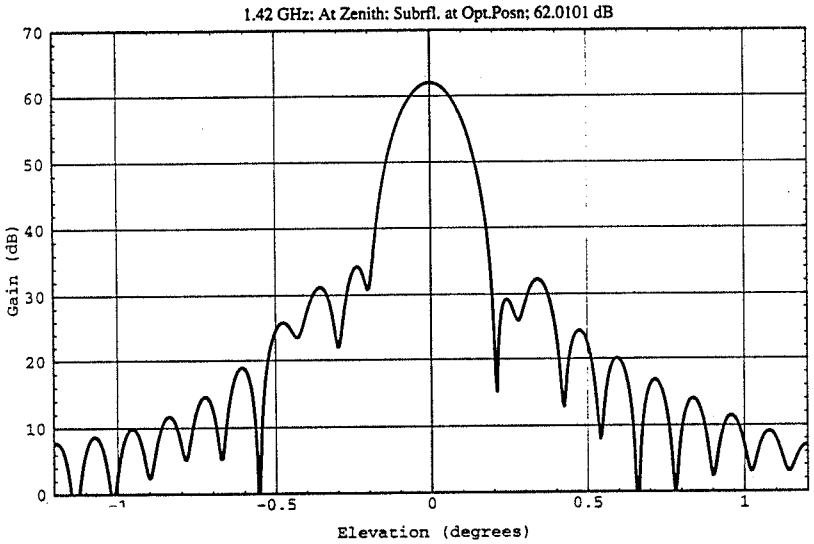

(a) 1.42 GHz

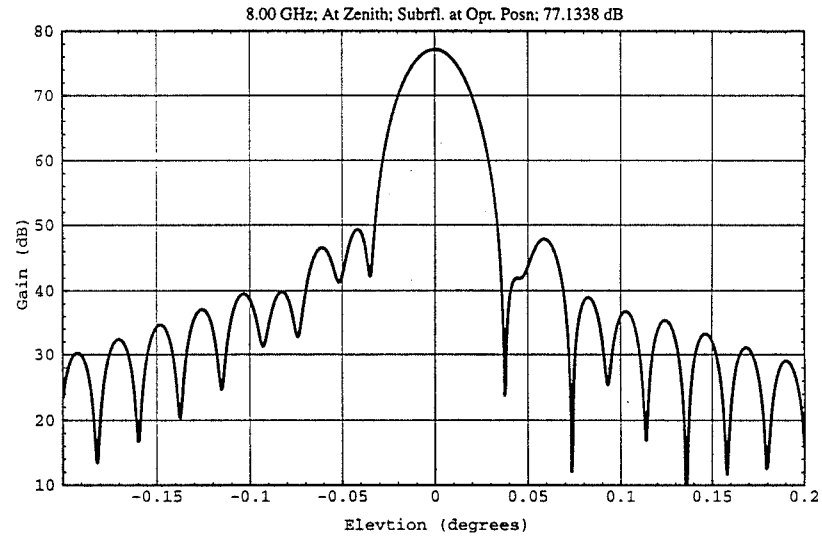

(b) 8.00 GHz

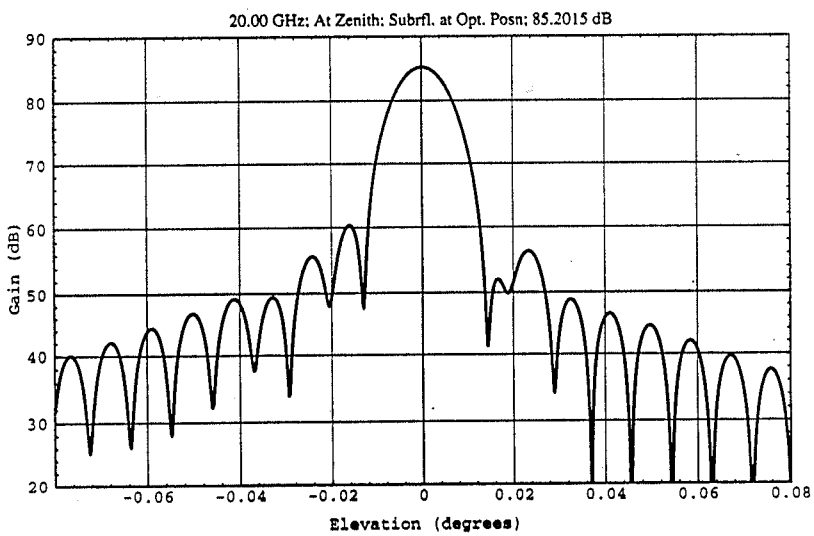

(c) 20.00 GHz

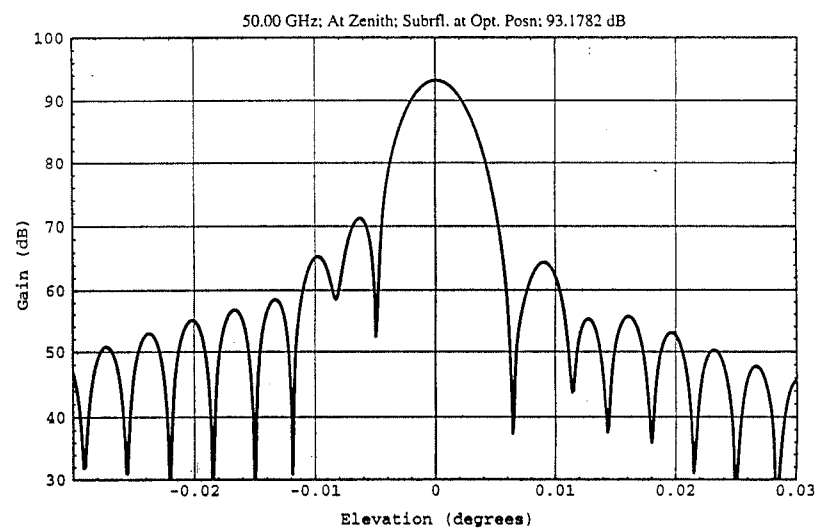

(d) 50.00 GHz

Fig. 9. Far-field patterns in the symmetric plane at zenith after correction.